DIFFERENTIAL AND INTEGRAL CROSS SECTIONS FOR THE LOSS AND CAPTURE OF ELECTRONS BY SINGLY CHARGED ARGON IONS AT 250—1400 keV ENERGIES

L. I. PIVOVAR, M. T. NOVIKOV, and V. M. TUBAEV

Physico-technical Institute, Academy of Sciences, Ukrainian S.S.R.

Submitted to JETP editor July 20, 1963

Measurements were made of the energy and angular dependences of the distribution of the charged fractions in a beam of argon particles undergoing single collisions with argon and krypton atoms. The data obtained agree with the Russek-Thomas theory. Measurements were made also of the differential effective cross sections for scattering and electron loss, and of the integral cross sections for the loss and capture of electrons by singly charged argon ions in argon and krypton. The measurements were made in the angular range 0—3°. Parts of the integral effective cross sections, corresponding to the scattering of the primary ions within the angular range 0—1°, were measured directly.

1. INTRODUCTION

THE processes of scattering accompanying the inelastic collisions of ions with gas molecules, in particular the "stripping" of electrons, were first studied by Fedorenko[1] and then by Kaminker and Fedorenko.[2] Later Everhart et al.[3,4] investigated the processes of scattering of several types of ion which were "stripped" in gases.

Basing themselves to a considerable extent on the work referred to above, Russek and Thomas[5] developed a phenomenological theory of ion-atom collisions leading to electron loss. The probabilities of the formation of the various charged fractions calculated by Russek and Thomas were in reasonable agreement with the experimental results of the cited work. However, we must bear in mind the fact that some of the initial assumptions were made by Russek and Thomas in such a way as to obtain the best agreement with these experimental data. Measurements of the angular distribution allow us not only to study the nature of the interaction of the particles in various inelastic processes but also to determine the true values of the integral cross sections of such processes as, for example, the electron loss by an ion or atom shell.

In recent years, several measurements have been made of the integral effective cross sections for the loss and capture of electrons by various ions during collisions with gaseous atoms and molecules. These measurements were carried out mainly at relatively high ion velocities.[6-8] Since, at high ion velocities, the process of elec-

tron loss is in the nature of an impact interaction between individual electrons and target atoms, the influence of the scattering on the measured cross sections should not be great. However, for ion velocities $v \leq 10^8$ cm/sec, the influence of the scattering of ions on the results of the measurements of the integral cross sections for the electron loss may be enormous. Thus, for example, Kaminker and Fedorenko[2] showed that the integral effective cross sections for the stripping, measured for ions which are little deviated, may be many times smaller than the corresponding cross sections measured with allowance for the angular distribution of the primary ions. Similar results were later reported in [3,4] The latter investigations, in which the angular distributions were allowed for, were carried out at ion energies not exceeding 180 keV.

Obviously, a study of the processes of the electron loss with allowance for the angular distribution carried out over a wider range of energies is of interest in determining the true integral effective cross sections and in further development of the ideas about the mechanism of the interaction of heavy atoms. In the present work, we determined the charged fractions in a beam of argon particles undergoing single collisions with argon and krypton atoms. We measured also the differential cross sections for scattering with electron loss and determined the integral cross sections for electron loss and capture by singly charged argon ions in argon and krypton. The measurements were carried out in the energy range 250—1400 keV and the angular range 0—3°.
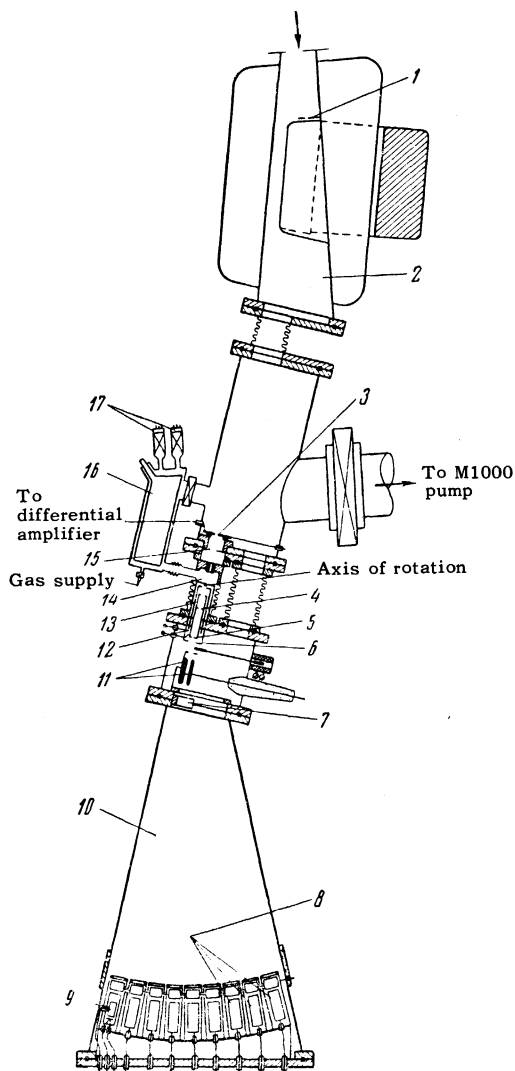
FIG. 1. Diagram of the apparatus.

2. EXPERIMENTAL APPARATUS AND MEASUREMENT METHOD

A beam of argon ions was obtained and accelerated by means of the electrostatic accelerator described earlier by the present authors.[9] The diagram of the apparatus used to carry out the measurements described below is given in Fig. 1.

A magnetic mass monochromator 2 was used to extract, from the ion beam produced by the accelerator, a uniform beam of singly charged argon ions and to direct this beam to a scattering chamber 14 through slits 3 and 15. The constancy of the beam direction and its parallelism were ensured by two rectangular slits 1 and 3. The slits 3, which was assembled from two halves insulated from each other, was used as the sensing unit for the stabilization of the accelerator voltage and for the simultaneous automatic maintenance of the ion

beam direction. At given values of the ion energy and the corresponding magnetic field in the monochromator, the beam could be kept accurately parallel. The slit 15, 3.5 mm long and 1.2 mm wide, was placed directly in front of the scattering chamber channel. The angle of the scattered beam of particles was varied by rotating an electrostatic analyzer 10 with respect to a fixed axis of rotation passing through the middle of the scattering chamber.

The beam of ions scattered through a given angle was selected by two narrow slits 4 and 5, 0.55 and 7 mm wide, respectively. The distance between these slits was 90 mm and the distance from the center of rotation to the slit 5 was 160 mm. The divergence of the scattered beam in the transverse direction was $\Delta\theta = \pm 0.5°$. The primary beam current in the scattering chamber was measured by a trap 13, connected to the system of collimating slits 4 and 5. To avoid distortion of the values of the primary current, measures were taken to suppress the secondary electrons by means of an electrode 12, and the outside surface of the trap was protected by a screen 6. The ion beam selected by the slits was directed to the electrostatic analyzer 10. The beams with different ion charges were separated by the electric field of a capacitor 11.

Receivers 8 were intended for the measurement of the intensities of the charged components of the beam with ion charges from +1 to +8. They were Faraday cups with guard electrodes for the suppression of the secondary electron emission. The positive plate of the capacitor was connected to the casing and therefore some of the electrons formed in the path of the beam may have been accelerated in the direction of the receivers 8, producing undesirable background. To eliminate this a permanent magnet 7, the field of which turned the electrons to the wall of the analyzer, was placed between the capacitor and the receivers.

The ion beams entering the receivers 8 were measured with vacuum-tube electrometers of $\approx 10^{-14}$ A/division sensitivity. The intensity (the number) of fast neutral atoms, formed by the capture of electrons by argon ions, was determined with a detector 9, working on the principle of measuring the current of the secondary electron emission due to the bombardment with fast argon atoms. The construction of this detector was the same as that of the detector used by us in another project. [10] To reduce the background due to the residual gases, a trap 16, filled with liquid nitrogen, was placed in the scattering chamber. The residual gas pressure in the scattering chamber was of

the order of $(2-4) \times 10^{-6}$ mmHg. High vacuum was established in the apparatus by oil diffusion pumps provided with traps cooled by liquid nitrogen. The pressure in the apparatus did not exceed $(2-3) \times 10^{-6}$ mm Hg. The gas pressure in the scattering chamber was measured with a manometer tube LM-2, denoted by 17 in Fig. 1, calibrated by means of a McLeod gage. The calibration was checked from time to time during the measurements. The initial data were the measured intensities of the ion beam components. Each component of the beam, beginning with that of zero charge and ending with that of octuply charged ions, was measured by a separate receiver.

To determine the range of pressures which would ensure single collisions, we investigated the dependence of the ratios of the currents of particles which underwent charge exchange to the primary current, as a function of the pressure in the scattering chamber. The curves of the dependences of J^{n+}/J_0 on p were recorded for various energies and angles of deviation. During the measurements of the cross sections, the range of pressures in the scattering chamber was selected each time so that a linear dependence of J^{n+}/J_0 on p was retained for the component with the highest ion charge, since for these ions the deviation from linearity occurred at relatively lower pressures, because of the higher probability of electron capture by multiply charged ions compared with the electron loss. The total differential cross sections for the scattering of primary ions σ^* into a unit solid angle, the scattering angle being θ in the laboratory system of coordinates, were determined using the formula

$$\sigma^* = d\sigma/d\omega = \sum_{k=1}^{8} N^k/N_0 mL\omega. \tag{1}$$

Here, N^k is the total flux of particles scattered through the angle θ, the charges of the particles being from $+1$ and $+8$, with the exception of the particles scattered on the residual gas in the scattering chamber. This particle flux was measured by the receivers 8. N_0 is the intensity of the primary beam of singly charged ions, measured with the receiver 13; m is the concentration of the target gas atoms with allowance for the residual pressure in the scattering chamber; L is the effective length of the target along the direction of the primary beam, determined by the geometry of the collimating slits and the angle θ; ω is the solid angle considered here, which is also determined by the geometry of the collimating slits and the dimensions of the slits of the receivers 8. The calculation of the quantity L was carried out in

the same way as in [2,4]. It is evident from Eq. (1) that the intensity of the neutral particle beam was neglected. This is because, even at the lowest investigated ion energies and the lowest scattering angles ($\theta = 1°$), the intensity of the fast-atom beam was negligibly small.

The differential cross sections for the loss of $(n-1)$ electrons were determined from the relationship

$$\sigma_{1n}^* = \sigma^* N \Big/ \sum_{k=1}^{8} N^k, \tag{2}$$

where N is the flux of particles of charge n, scattered through the angle θ, measured by the appropriate receiver, with the exception of the particles scattered on the residual gas in the scattering chamber. The parts of the total effective cross section for the electron loss in the angular range $1-3°$ were calculated by integrating the differential cross sections for the processes considered in solid angle elements. The appropriate integral can be written in the form

$$\sigma_{1n}(1 \div 3°) = 2\pi \int_{1°}^{3°} \sigma_{1n}^*(\theta) \sin\theta d\theta. \tag{3}$$

To integrate, we plotted the curves of the dependence $\sigma_{1n}^*(\theta)$ for given values of the ion energy, and the integrals were obtained graphically.

To measure the parts of the total cross sections for the capture and loss of electrons corresponding to the angular range $0-1°$, we altered the collimating system of the scattering chamber in such a way that circular slits selected a beam in the shape of a cone with the plane angle at its vertex equal to $2°$. The dimensions of the circular apertures of the receivers 8 ensured complete collection of all the particles scattered through the angles from 0 to $1°$. The parts of the cross sections, $\sigma_{1n}(0-1°)$, were calculated using the formula

$$\sigma_{1n}(0 \div 1°) = N/N'mL, \tag{4}$$

where N is the flux of particles of charge n, with the exception of the particles formed in the residual gas and at the edges of the slits; N' is the intensity of the primary particle beam; L is the effective length of the scattering chamber. To check the possible influence of the dimensions of the collimating slits and the entry slits of the receivers, control measurements of the differential cross sections were carried out by varying the dimensions of the slits. It was found that the results of the measurements were unaffected, within the limits of the experimental error, by considerable variations of the dimensions of the collimating and receiver slits.

3. RESULTS OF MEASUREMENTS AND DISCUSSION

We investigated the processes of scattering, capture and loss of electrons, by singly charged argon ions on collision with argon and krypton atoms. The gases used as targets contained impurities in amounts not greater than 0.1%.

a) Distribution of the Charged States in the Beam. Figures 2 and 3 give the charge distributions of the argon ions for single collisions in argon and krypton as a function of the energy for the scattering angles θ, in the laboratory system, of 1, 2 and 3°. These figures show that in the case of some charged states the curves have maxima, which are displaced toward higher energies on increase of the number of stripped electrons. These observations may be explained by the fact that since a higher charge of the ion corresponds to a relatively higher energy loss, it is obvious that, with increase of the relative velocity of the ions, the role of the processes involving greater energy loss increases.

On increasing the scattering angle, the $F_n(E)$ curves become steeper, and their maxima become narrower and shift toward lower energies. This
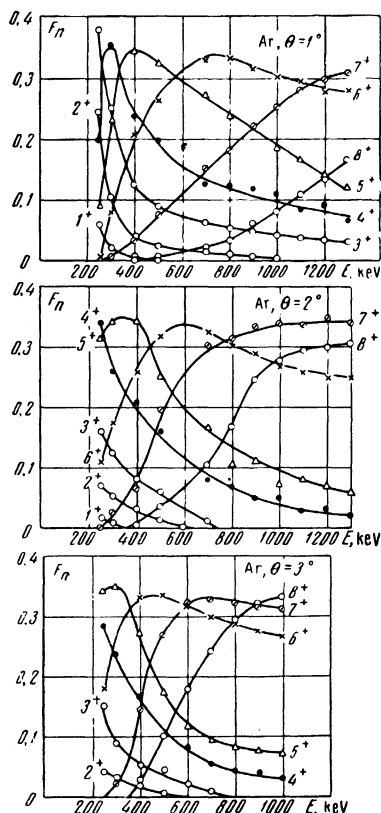
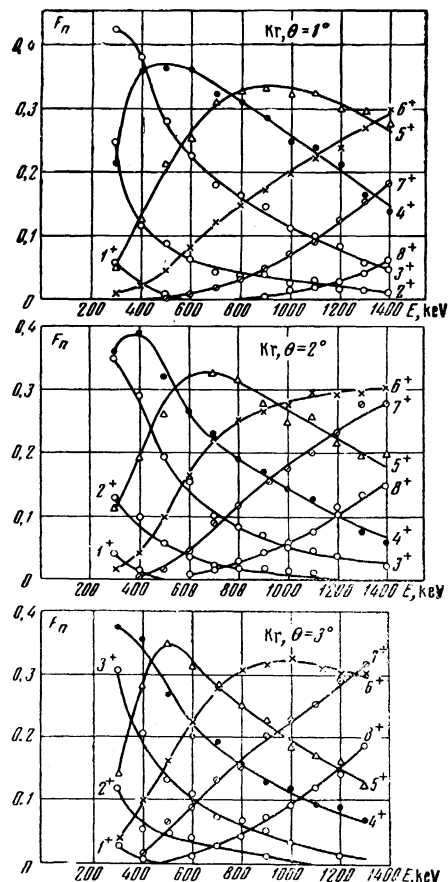FIG. 3. Dependence of the distribution of the charged fractions on the energy of argon ions in krypton.

FIG. 2. Dependence of the distribution of the charged fractions on the energy of argon ions in argon.

nature of the dependence of these curves on the scattering angle is an additional confirmation of the explanation given above, because large scattering angles correspond to relatively closer approach of the particles and consequently stronger transfer of energy to the inelastic interactions.[11] The difference between the curves obtained in argon and krypton is this: the curves representing the same number of lost electrons are shifted toward lower energies in argon compared with the corresponding curves for krypton. This indicates that the relative transfer of the inelastic energy for the stripping of an argon ion in krypton is less than in argon.

The results of the measurements of the charged fractions, given in Figs. 2 and 3, allow us to make a direct comparison of these results with the distributions of the charged fractions calculated by Russek and Thomas.[5] It follows from their theory that the amplitudes of the maxima and the intersections of the curves are independent of the energy and the scattering angle, and are governed only by the charged states corresponding to the given maxima or intersecting curves. A compari-

Table I

Maxima and intersections of curves	Target gas AR			Target gas Kr			Theoret. values
	$\theta = 1°$	$\theta = 2°$	$\theta = 3°$	$\theta = 1°$	$\theta = 2°$	$\theta = 3°$	
$F_1 \times F_5$	—	—	—	0.05	—	—	—
$F_1 \times F_6$	0.03	—	—	0.02	0.02	—	0.02
$F_2 \times F_4$	0.23	—	—	0.23	—	—	0.25
$F_2 \times F_5$	0.15	—	—	0.13	0.12	—	0.13
$F_2 \times F_6$	0.09	—	—	0.07	0.07	0.07	0.07
$F_2 \times F_7$	0.04	0.04	0.03	0.04	0.04	0.05	0.03
$F_2 \times F_8$	0.02	0.02	0.02	0.02	0.02	0.03	—
$F_3 \times F_4$	0.33	—	—	0.36	—	—	0.35
$F_3 \times F_5$	0.24	—	—	0.25	—	—	0.24
$F_3 \times F_6$	0.16	0.15	—	0.15	0.15	0.15	0.15
$F_3 \times F_7$	0.08	0.08	0.07	0.1	0.09	0.09	—
$F_3 \times F_8$	0.05	0.05	0.05	0.05	0.05	0.05	—
F_4	0.35	—	—	0.37	0.39	—	0.37
$F_4 \times F_5$	0.32	0.32	—	0.32	0.31	0.32	0.32
$F_4 \times F_6$	0.23	0.23	0.24	0.23	0.22	0.22	0.24
$F_4 \times F_7$	0.14	0.16	0.16	0.16	0.15	0.16	—
$F_4 \times F_8$	0.1	0.1	0.1	—	0.1	0.1	—
F_5	0.34	0.35	0.34	0.34	0.33	0.35	0.35
$F_5 \times F_6$	0.3	0.3	0.31	0.28	0.28	0.28	—
$F_5 \times F_7$	0.22	0.22	0.22	—	0.23	0.21	—
$F_5 \times F_8$	0.14	0.15	0.14	—	—	0.15	—
F_6	0.34	0.34	0.33	—	—	0.32	—
$F_6 \times F_7$	0.29	0.31	0.32	—	—	0.3	—
$F_6 \times F_8$	—	0.28	0.29	—	—	—	—
F_7	—	—	0.33	—	—	—	—

son of the amplitudes of the maxima and the heights at which the curves intersect is made in Figs. 2 and 3 for the angles θ, equal to 1, 2, and 3°. The results of this comparison, and also of a comparison with the theoretical data, are collected in Table I.

Table I shows that the amplitudes of the maxima and the heights of the intersections of the curves representing the charge distribution for the angles 1, 2, and 3° nearly coincide with the amplitudes and heights calculated theoretically. In all cases, the difference does not exceed 0.02— 0.03 for peak heights of 0.35—0.4. Therefore, the agreement between experiment and theory can be regarded as good. We note also that the theoretical predictions are satisfied well both in argon and in krypton.

b) Differential and Integral Cross Sections for Electron Capture and Loss. Figure 4 gives the experimental data representing the dependence of the total differential cross section for the scattering of argon ions on their energy, for collisions with argon and krypton atoms leading to the scattering through the angles $\theta = 1$—3° in the laboratory system. In the same figure, the continuous lines represent the dependence of the total differential scattering cross section calculated on the assumption [12] that the elastic interaction between the particles can be described by a screened Coulomb potential of the type

$$U(r) = (Z_1 Z_2 q^2 / r) \exp(-r/a), \qquad (5)$$

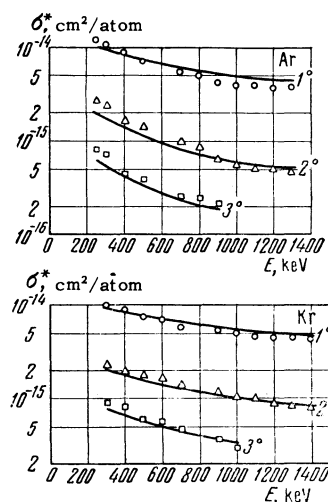where $Z_1 q$ and $Z_2 q$ are the charges of the nuclei

FIG. 4. Energy dependences of the total differential cross sections for the scattering of argon ions in argon and krypton for $\theta = 1 - 3°$.

of the interacting particles; the screening parameter is $a = a_0 / \sqrt{Z_1^{2/3} + Z_2^{2/3}}$. Comparison of the experimental and calculated data shows that they are in agreement over the whole range of the investigated energies. The observed difference between the experimental and calculated results is within the limits of the experimental error.

Using the data on the total scattering cross sections and the data on the values of the charged fractions, we calculated the differential cross sections $\sigma_{11}^* - \sigma_{18}^*$ by means of Eq. (2). Figures 5 and 6 give the dependences of the differential cross
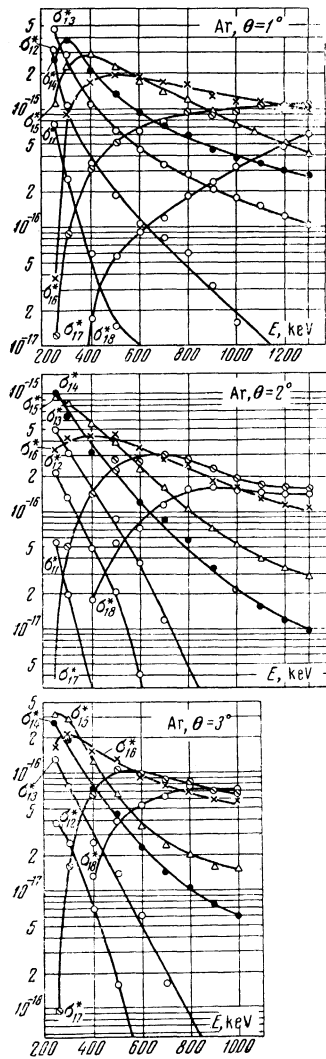
FIG. 5. Dependence of the differential cross sections σ^*_{in} in argon on the energy of argon ions for $\theta = 1 - 3°$.

sponding to the angular range 1—3°, we plotted the curves of the dependence $\sigma^*_{in}(\theta)$ from the data of Figs. 5 and 6. These curves, plotted for the energies from 250 keV to 1400 keV in steps of 100 keV, were used to carry out the integration. The parts of the total cross sections for the electron loss calculated in this way for the angular range 1—3° are listed for argon ions in argon in Table II, and for argon ions in krypton in Table III. The same tables give the results of the direct measurements of the parts of the effective cross sections for the electron loss corresponding to the angular range 0—1°. These tables show that the parts of the cross sections for the electron loss σ_{in}, corresponding to the angular range 0—1°, rise with increase of the ion energy and that the slope of this rise increases with increase of the number of stripped electrons.

sections σ^*_{in} on the energy of argon ions for the scattering angles $\theta = 1$—3° in argon and krypton. It is evident from these figures that the higher ion charges correspond to less steep slopes of the dependences $\sigma^*_{in}(E)$. In the case of some of the charged states, the curves pass through maxima. With increase of the number of lost electrons, these maxima shift toward higher energies. These features may be explained in the same way as in the case of the dependence of the charged fractions on the ion energy.

The nature of the curves giving the dependences of the differential cross sections σ^*_{in} on the energy and the scattering angle is approximately the same in argon and krypton. However, in argon all the curves are displaced toward lower energies compared with krypton.

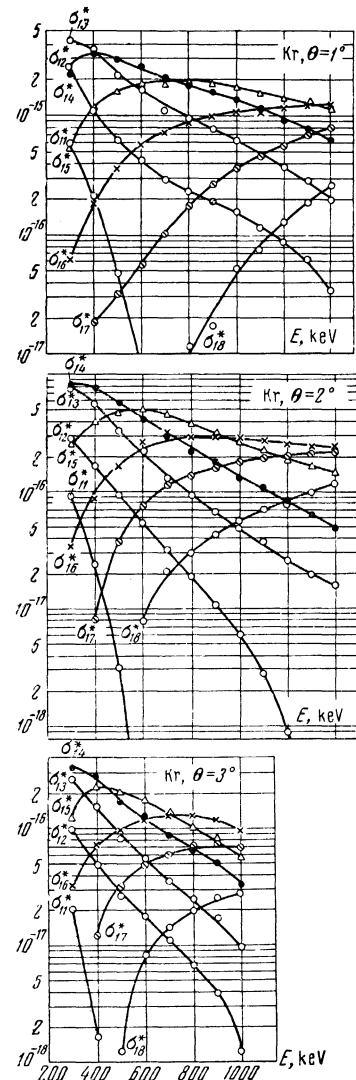To calculate the parts of the total effective cross sections for the electron stripping, corre-

FIG. 6. Dependence of the differential cross sections σ^*_{in} in krypton on the energy of argon ions for $\theta = 1 - 3°$.

Table II. Parts of the total cross sections σ_{1n} in the angular ranges $\theta = 0-1°$ and $\theta = 1-3°$ in argon (cross sections are given in units of 10^{-18} cm²/atom)

E, keV	σ_{11} 1—3°	σ_{12} 0—1°	1—3°	σ_{13} 0—1°	1—3°	σ_{14} 0—1°	1—3°	σ_{15} 0—1°	1—3°	σ_{16} 0—1°	1—3°	σ_{17} 0—1°	1—3°	σ_{18} 1—3°
250	—	—	5.6	—	9.15	—	8.5	—	6.14	—	1.79	—	0.032	—
300	1.3	248	2.16	70.5	5.55	12.7	6.6	1.7	7.76	0.26	3.47	—	0.37	—
400	0.47	274	0.73	91.5	22	15.9	4.32	3.16	6.78	0.68	4.7	—	1.25	0.13
500	—	349.6	0.36	128.5	1.36	27	2.92	5.1	5.07	1.9	4.91	0.2	2.32	0.4
600	—	379	0.18	139.1	0.84	32.1	1.91	8.2	3.58	2.65	4.43	0.47	2.5	0.57
700	—	400	—	150.5	0.55	41.6	1.44	9.0	2.8	3.85	4.0	0.87	2.7	0.79
800	—	430	—	160	—	45.9	1.16	10.2	2.33	4.2	3.65	1.28	2.8	1.08
900	—	430	—	175	—	51.2	0.81	11.45	1.65	5	2.77	1.86	2.40	1.16
1000	—	420	—	177	—	50.3	0.67	14.15	1.35	5.9	2.47	2.37	2.39	1.28
1100	—	420	—	192	—	58.4	0.58	16.4	1.106	7.3	2.22	2.84	2.38	1.32
1200	—	420	—	191.5	—	60.5	0.49	18.1	0.9	7.5	1.02	3.45	2.36	1.39
1300	—	410	—	191.5	—	67.6	0.42	19.05	0.75	8.0	0.62	3.7	2.4	1.53

Table III. Parts of the total cross sections σ_{1n} in the angular ranges $\theta = 0-1°$ and $\theta = 1-3°$ in krypton

E, keV	σ_{11} 1—3°	σ_{12} 0—1°	1—3°	σ_{13} 0—1°	1—3°	σ_{14} 0—1°	1—3°	σ_{15} 0—1°	1—3°	σ_{16} 0—1°	1—3°	σ_{17} 1—3°	σ_{18} 1—3°
300	1.34	234.8	5.2	40.7	10.1	4.05	7.27	—	2.42	—	0.29	—	—
400	0.57	287.6	2.43	62.2	7.8	8.63	8.63	0.98	3.92	—	0.8	0.09	—
500	0.086	318.6	1.38	76.2	4.78	15.3	7.1	1.9	4.87	0.21	1.42	0.28	—
600	—	379.1	0.89	112.6	3.41	20.6	5.8	5.0	5.3	0.585	2.23	0.51	0.063
700	—	339.4	0.59	119.7	2.29	21.6	4.5	5.3	5.0	0.93	4.37	0.76	0.126
800	—	359.6	0.445	123.1	1.86	23.25	3.75	5.35	4.65	1.46	2.83	0.98	0.19
900	—	449.65	0.347	148.5	1.48	30.8	3.2	7.6	4.32	1.95	2.98	1.24	0.26
1000	—	439.74	0.258	154.0	1.13	32.3	2.68	7.9	3.83	2.04	2.95	1.44	0.374
1100	—	479.8	0.184	159.1	0.887	38.84	2.16	9.35	3.39	2.35	2.77	1.62	0.48
1200	—	459.9	0.133	164.3	0.664	44.2	1.77	10.0	2.95	2.6	2.89	1.77	0.6
1300	—	480.0	—	189.5	0.51	50.57	1.43	12.33	2.67	3.6	2.96	1.97	0.853
1400	—	520.0	—	219.56	0.44	52.77	1.23	16.45	2.55	4.65	2.76	2.6	1.06

In the angular range 1—3°, the nature of the energy dependence of σ_{1n} is more complex and is governed to a great extent by the number of stripped electrons. For small numbers of stripped electrons, the cross section $\sigma_{1n}(1-3°)$ decreases with increase of the ion energy. For large numbers of stripped electrons, the same cross section passes through a maximum or rises monotonically with increase of the energy. The energies at which the maxima occur increase with increase of the number of stripped electrons. The measured effective cross sections σ_{10} for the capture of an electron by a singly charged argon ion in the angular range 0—1° may be regarded as the total cross sections because the accompanying scattering of ions through angles larger than 1° was found to be very weak over the whole investigated range of energies.

Using the data in Tables II and III and taking into account the cross sections for which there is a very rapid reduction of the dependence $\sigma_{1n}^{*}(\theta)$ within the limits 1—3°, we can easily determine the total effective cross sections for the electron loss in the form of the sum $\sigma_{1n}(0-1°) + \sigma_{1n}(1-3°)$. These cross sections can be regarded as total without committing a large error because the contribution due to the scattering of ions through

angles > 3° is slight. The total cross sections obtained in this way for the electron loss σ_{1n} are given in Fig. 7. In the range of energies investigated by us, there are no published data with which our results could be compared directly. Therefore Fig. 7 presents data taken from [2-4] for low energies in argon, and from [6-8] for points at 1400 keV. Figure 7 shows that the published data for low energies and our results can be fitted to the same monotonic curves. At high energies, our results match the data reported in [6-8].

It is easily seen that in the investigated range of energies the effective cross sections for the electron capture σ_{10} decrease monotonically with increase of the ion energy. The effective cross sections for the electron loss increase with increase of the ion energy, with the maxima of the cross sections σ_{12} and σ_{13} in argon being reached at the energies of 1000—1200 keV. The nature of the dependences $\sigma_{1n}(E)$ was approximately the same in argon and krypton, but, as in the case of the differential cross sections, the maxima of the cross sections σ_{1n} for the electron loss were displaced toward high energies in krypton compared with argon. A possible reason for this is given above, in the consideration of the dependences of
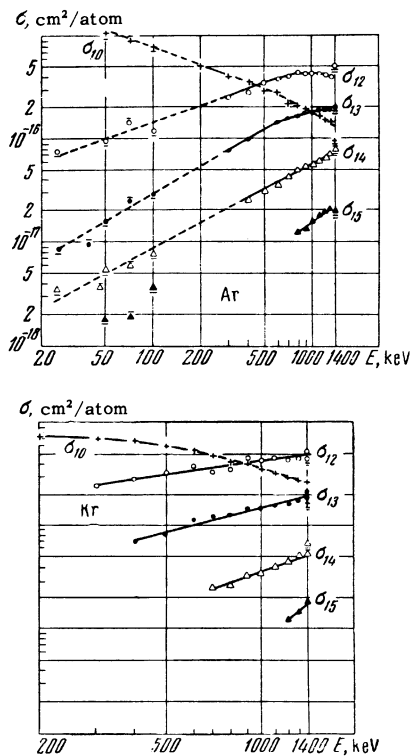
$\mathscr{C}$, cm^2/atom

$\mathscr{C}$, cm^2/atom

FIG. 7. Energy dependences of the total cross sections for the capture σ_{10} and loss σ_{1n} of electrons by argon ions in argon and krypton. The points marked with a bar above were taken from [2]; those with a bar below are from [4]; and those with two bars below are from [5-8].

the charged fractions on the energy in argon and krypton.

In conclusion, it is our pleasant duty to thank A. K. Val'ter, Academician of the Ukrainian Academy of Sciences, for his interest and the operators

of the accelerator, K. M. Khurgin and V. G. Rubashko, for their help in the measurements.

[1] N. V. Fedorenko, ZhTF 24, 784 (1954).

[2] D. M. Kaminker and N. V. Fedorenko, ZhTF 25, 2239 (1955).

[3] Fuls, Jones, Ziemba, and Everhart, Phys. Rev. 107, 704 (1957).

[4] Jones, Ziemba, Moses, and Everhart, Phys. Rev. 113, 182 (1959).

[5] A. Russek and M. T. Thomas, Phys. Rev. 109, 2015 (1958).

[6] Nikolaev, Dmitriev, Fateeva, and Teplova, JETP 40, 989 (1961), Soviet Phys. JETP 13, 695 (1961).

[7] Dmitriev, Nikolaev, Fateeva, and Teplova, JETP 42, 16 (1962), Soviet Phys. JETP 15, 11 (1962).

[8] Dmitriev, Nikolaev, Fateeva, and Teplova, JETP 43, 361 (1962), Soviet Phys. JETP 16, 259 (1963).

[9] L. I. Pivovar and V. M. Tubaev, ZhTF 32, 713 (1962), Soviet Phys. Tech. Phys. 7, 520 (1962).

[10] Pivovar, Tubaev, and Novikov, JETP 41, 26 (1961), Soviet Phys. JETP 14, 20 (1962).

[11] N. V. Fedorenko, UFN 68, 481 (1959), Soviet Phys. Uspekhi 2, 526 (1960).

[12] Everhart, Stone, and Carbone, Phys. Rev. 99, 1287 (1955).

68